Published in final edited form as:
Hear Res. 2014 October ; 316: 82–93. doi:10.1016/j.heares.2014.07.011.

Factors associated with Hearing Loss in a Normal-Hearing Guinea Pig Model of Hybrid Cochlear Implants

Chiemi Tanaka, Ph.D.[1], **Anh Nguyen-Huynh, M.D., Ph.D**, **Katherine Loera, B.S.**[1], **Gemaine Stark, B.S.**, and **Lina Reiss, Ph.D.**
Oregon Hearing Research Center, Department of Otolaryngology, Mail Code: NRC04, Oregon Health and Science University, 3181 SW Sam Jackson Park Road, Portland, OR 97239, USA

Anh Nguyen-Huynh: nguyanh@ohsu.edu; Katherine Loera: loerakatherine@gmail.com; Gemaine Stark: starkg@ohsu.edu; Lina Reiss: reiss@ohsu.edu

Abstract

The Hybrid cochlear implant (CI), also known as Electro- Acoustic Stimulation (EAS), is a new type of CI that preserves residual acoustic hearing and enables combined cochlear implant and hearing aid use in the same ear. However, 30-55% of patients experience acoustic hearing loss within days to months after activation, suggesting that both surgical trauma and electrical stimulation may cause hearing loss.

The goals of this study were to: 1) determine the contributions of both implantation surgery and EAS to hearing loss in a normal-hearing guinea pig model; 2) determine which cochlear structural changes are associated with hearing loss after surgery and EAS. Two groups of animals were implanted (n=6 per group), with one group receiving chronic acoustic and electric stimulation for 10 weeks, and the other group receiving no direct acoustic or electric stimulation during this time frame. A third group (n=6) was not implanted, but received chronic acoustic stimulation. Auditory brainstem response thresholds were followed over time at 1, 2, 6, and 16 kHz. At the end of the study, the following cochlear measures were quantified: hair cells, spiral ganglion neuron density, fibrous tissue density, and stria vascularis blood vessel density; the presence or absence of ossification around the electrode entry was also noted.

After surgery, implanted animals experienced a range of 0-55 dB of threshold shifts in the vicinity of the electrode at 6 and 16 kHz. The degree of hearing loss was significantly correlated with reduced stria vascularis vessel density and with the presence of ossification, but not with hair cell counts, spiral ganglion neuron density, or fibrosis area. After 10 weeks of stimulation, 67% of implanted, stimulated animals had more than 10 dB of additional threshold shift at 1 kHz,

Corresponding Author: Chiemi Tanaka, Ph.D. 677 Ala Moana Blvd., Suite 625, Honolulu, HI 96816, Department of Communication Sciences and Disorders, John A. Burns School of Medicine, University of Hawai'i at Mānoa, Phone: +1-808-692-1585, Fax: +1-808-566-6292, tanakach@hawaii.edu.
[1]Present Address: 677 Ala Moana Blvd., Suite 625, Honolulu, HI 96816, Department of Communication Sciences and Disorders, John A. Burns School of Medicine, University of Hawai'i at Mānoa

Conflict of Interest: The authors declare that we have no conflict of interest.

compared to 17% of implanted, non-stimulated animals and 0% of non-implanted animals. This 1-kHz hearing loss was not associated with changes in any of the cochlear measures quantified in this study. The variation in hearing loss after surgery and electrical stimulation in this animal model is consistent with the variation in human patients. Further, these findings illustrate an advantage of a normal-hearing animal model for quantification of hearing loss and damage to cochlear structures without the confounding effects of chemical- or noise-induced hearing loss. Finally, this study is the first to suggest a role of the stria vascularis and damage to the lateral wall in implantation-induced hearing loss. Further work is needed to determine the mechanisms of implantation- and electrical-stimulation-induced hearing loss.

Keywords

Cochlear implant; Hybrid; EAS; hearing loss; guinea pig; stria vascularis

1. Introduction

Hearing aids (HAs) and cochlear implants (CIs) have become highly successful treatments for hearing loss (HL) and deafness. While these devices benefit many individuals by improving speech recognition, some limitations still exist. For example, high-frequency sensorineural HL is the most common type of HL observed in the clinic, but clinical reports and literature indicate that providing high-frequency amplification in these patients does not always restore speech understanding (Pavlovic et al., 1984; Kamm et al., 1985; Ching et al., 1998; Hogan and Turner, 1998). At the same time, these patients typically do not qualify for full-insertion CIs because they have too much residual hearing.

The Hybrid CI, also known as electric and acoustic stimulation (EAS), was developed to address the above limitations of the HAs and CIs for these patients (Kiefer et al., 2002; Gantz and Turner, 2003). This is a new type of CI that preserves residual hearing and enables patients to use a hearing aid in the same ear with the cochlear implant after implantation. The use of a shorter, thinner CI electrode array makes it possible to reduce implantation trauma in the low-frequency region of the cochlea, since the array is only inserted into the basal to middle part of the cochlea, leaving the apical cochlea intact. When “soft” surgery techniques are used, low-frequency residual hearing can be preserved. In addition to improving speech recognition in quiet, the Hybrid CI allows patients to perform better in speech recognition in competing background noise (Wilson et al., 2003; Turner et al., 2004, 2008) and musical melody recognition (Gfeller et al., 2006) compared to full insertion CI patients.

However, optimum benefit from Hybrid CIs depends on preservation of residual hearing within the implanted ear. Gantz et al. (2009) reported that 30% of Cochlear Nucleus Hybrid CI recipients had greater than 30 dB of mean low-frequency threshold shifts postoperatively. In their study, HL occurred at different time points ranging from between surgery and CI activation to within 3-36 months after CI activation. Similarly, Gstoettner et al (2009) reported that 55.6% of the Med-EL Flex EAS recipients (5 out of 9 subjects) showed greater than 10 dB elevations in average pure-tone thresholds from 125 to 750 Hz between 1 month and 17 months after implantation. Santa Maria et al. (2013) also reported progressive

changes in hearing preservation over time after implantation. At 0-3 months after implantation, complete, partial, and minimal hearing preservation rates were reported as 42.9%, 50%, and 7.1%, respectively. However, several months after implantation, hearing preservation rates decreased to 22.2%, 66.7%, and 11.1% at 6-12 months and 25%, 12.5%, and 37.5% at 12 to 24 months after implantation, respectively. These study results suggest that the residual HL can occur anytime after implantation and may be delayed effects of surgical trauma and/or electrical stimulation delivered by the Hybrid CI into the cochlea.

Potential mechanisms of delayed HL related to surgical trauma include direct mechanical trauma to the basilar membrane or osseous spiral lamina (Briggs et al., 2005; O'Leary et al., 1991; Roland and Wright, 2006), or an inflammatory or immune response leading to hair cell death (Eshraghi et al., 2013). Another possibility which has been under-investigated is damage to the lateral wall and the stria vascularis (SV) which could lead to threshold shifts via a reduced endocochlear potential (Wright and Roland, 2013). The formation of fibrosis or new bone growth after implantation can also theoretically cause HL by attenuating the traveling wave (Choi and Oghalai, 2005), and a significant but small correlation has been reported between fibrosis and ABR thresholds (O'Leary et al. 2013).

Another possibility is that electrical stimulation itself contributes to residual HL after implantation. There are few published studies that have directly looked at residual hearing changes with electrical stimulation. Kang et al. (2010) measured residual hearing changes with cochlear implantation and electrical stimulation in both normal-hearing and chemically-deafened guinea pigs, as part of a study looking at electrical stimulation efficacy rather than residual HL. They reported that one of the implanted normal-hearing guinea pigs showed postoperative hearing threshold elevations at 8 and 24 kHz (lower frequencies were not tested), but no corresponding hair cell or spiral ganglion cell pathology. Coco el al. (2007) measured hearing thresholds after long-term cochlear implantation and electrical stimulation in chemically-deafened cats. Electrical stimulation was delivered via a CI for 6 hours per day for 5 days per week for up to 252 days. Interestingly, partially deafened animals showed no significant change in acoustic hearing, which contradicts the results from Gantz et al. (2009) in Hybrid CI patients. However, the Coco et al. study (2007) stimulation protocol differed from clinical Hybrid programming in two key ways: electrical stimulation parameters were fixed rather than updated periodically during the experimental period, and electrical stimulation was provided alone without acoustic stimulation.

The goals of this study were to: 1) determine the contributions of both implantation surgery and EAS to hearing loss in a normal-hearing guinea pig Hybrid CI model; 2) determine which cochlear structural changes are associated with hearing loss after surgery and EAS. An animal model was used to reduce the heterogeneity seen in human Hybrid CI patients due to differences in genetic composition, age, medical history, and medication usage, which can confound the interpretation of data, and to allow timely investigation of cochlear structural changes after hearing loss. Guinea pigs serve as an excellent Hybrid CI animal model since their cochleae are easily accessible and large enough to implant multiple electrodes in a commercially available electrode array (Kang et al., 2010). Normal-hearing instead of deafened animals were used to further reduce confounding effects of noise- or chemically-induced hearing loss on the histology. Finally, the chronic stimulation

parameters in this model were set up to simulate human Hybrid CI patients as closely as possible.

In this study, we found changes in hearing thresholds both after surgery and chronic acoustic and electric stimulation. Cochlear histology conducted at the conclusion of the study showed significant associations of implantation-induced hearing loss with stria vascularis blood vessel density and ossification, but not hair cell counts, spiral ganglion neuron density, or fibrosis area. No associations were observed for long-term hearing loss after stimulation with any of the histological measures.

2. Material and Methods

2.1 Subjects

Eighteen male, 6-week old albino Dunkin-Hartley guinea pigs were purchased from Charles River (Wilmington, MA). Average weight was 524.8 ± 61.9 g. All animal protocols were approved by the Oregon Health and Science University Committee on the Use and Care of Animals and veterinary care was provided by the Department of Comparative Medicine.

2.2 Research Design

Three groups of normal-hearing guinea pigs (n=18; n=6 per group) were studied in order to determine the effects of both implantation trauma and chronic electric and acoustic stimulation on hearing. The first group, the Chronic Acoustic Stimulation control group (CAS) consisted of non-implanted guinea pigs that received acoustic stimulation only. The second group, the No Stimulation (NS) group, underwent cochlear implantation, but received no direct acoustic or electric stimulation. The third group, the Chronic Acoustic and Electric Stimulation (CAES) group, underwent cochlear implantation and received combined acoustic and electric stimulation.

Figure 1 shows the study timeline. First, baseline auditory brainstem response (ABR) thresholds were obtained from all guinea pigs. All animals underwent gradual acclimation over 2 weeks to acoustic stimulation while in a restraint tube, starting from 15 minutes a day and increasing incrementally to 3 hours a day. Cochlear implant surgery was performed in the NS and CAES groups 2 weeks later at the age of 8 weeks. Implanted animals were allowed to recover for 2 weeks. ABRs and electrically-evoked ABRs (EABRs) were measured in the implanted animals (NS and CAES groups) at 2 and 4 weeks after the surgery. The animals in the non-implanted CAS group were also tested for ABRs at the same intervals as the other groups. At 5 weeks following implantation, the animals in the CAES group were programmed using a combination of electrophysiological testing (EABR) to measure thresholds (T-levels) and behavioral observation to measure maximum comfortable levels (C-levels). Chronic stimulation (3 hours/day) was initiated at 6 weeks after implantation and continued for 10 weeks for the CAS and CAES groups. All groups were placed in the restraint tube; the CAS group received only acoustic stimulation, the CAES group received acoustic and electric stimulation, and the NS group was placed in a separate room with no acoustic or electric stimulation. Biweekly ABRs and EABRs were performed to obtain thresholds. T-levels were adjusted if any changes were detected in the EABR thresholds, and C-levels were checked and changed weekly based on behavioral

observations. All animals were sacrificed at 16 weeks after implantation and cochleae were collected for histological analysis.

2.3 Cochlear implants

Standard 8-ring animal electrode arrays with a ball electrode (#Z60275, Cochlear Limited, Lane Cove, Australia) were used in the current study. These electrode arrays were chosen because they have the same chemical composition and assembly as the clinical CI electrodes. Five to seven of the electrodes were inserted into the scala tympani.

The diameter of the implant was 0.45 mm, and the centers of the electrodes were 0.75 mm apart. Three medical-grade stainless steel brackets with screw holes were attached to each encased receptacle in order to secure the receptacle on top of the skull with medical-grade stainless steel screws. All electrode array assemblies were autoclaved and cooled to room temperature before implantation.

2.4 Surgical Procedures

For all animals, the CI surgery was performed on the left ear.

The animals were anesthetized with ketamine (60 mg/kg) and xylazine (5 mg/kg) through intramuscular (IM) injection. Supplemental doses of anesthetics were given as necessary. The surgical area was shaved and aseptically prepared with 70% ethanol and Betadine. Local anesthesia (lidocaine 2 mg/kg) was injected subcutaneously (SC) along the intended incisions. The subjects were placed on a heating pad and rectal temperature was maintained around 37 °C. In addition to the temperature, vital signs (heart rate, respiratory rate, oxygen level, and pulse rate) were recorded using a vital signs monitor.

Surgery was performed as follows under a surgical microscope. Through a left postauricular incision, the left bulla was exposed and opened using a 1.4 mm acorn burr and rongeur to gain access to the round window niche. Through a midline skull incision, the CI connector was secured to top of the skull with three screws. The CI electrode array and ball electrode were tunneled along the skull underneath soft tissue into the left bulla. The ball electrode was then positioned under the left temporalis muscle. A cochleostomy was made just inferior and anterior to the round window using a 0.5 mm diamond burr. Through the cochleostomy, the CI electrode array was inserted into the scala tympani until slight resistance was felt. Between five to seven electrodes were inserted and the number of intracochlear electrodes was recorded for each animal. Based on the cochleostomy location, insertion angle, and insertion depth, the frequencies stimulated at the tip of the electrode in the cochlea were estimated to vary between 12-16 kHz (Greenwood, 1990). The cochleostomy was sealed with muscle plugs.

During this surgery, the right ear was mechanically deafened as follows: the right bulla was exposed through a right postauricular incision and opened to gain access to the round window niche. The round window and the basal turn of cochlea were opened and perilymph was thoroughly evacuated with suction. The purpose of mechanical deafening was to prevent bone-conduction cross-hearing effects from the non-implanted ear on ABR threshold estimates from the CI side. At 4 weeks after implantation, this deafening

procedure produced average ABR thresholds and SDs of >78.8±15.7 dB SPL at 1 kHz, >76.7±15.4 dB SPL at 2 kHz, >84.2±11.6 dB SPL at 6 kHz, and >83.8±12.1 dB SPL at 16 kHz. ABR thresholds from some animals exceeded the limit of the equipment (90 dB SPL) at 4 weeks after implantation, and by the end of the study, all animals developed ABR thresholds of 85 dB SPL or higher at all frequencies.

Upon completion of the skin closure, electrode impedance was measured using Cochlear Custom Sound software. Postoperatively, chloramphenicol sodium succinate (30 mg/kg, IM), buprenorphine (0.05 mg/kg, SC), and 5-ml warmed lactated ringers (SC) were given. Vitamin C (10 mg/kg, IM) was provided for three days postoperatively. Animals were kept warm and monitored until fully conscious, and allowed to recover for 2 weeks.

2.5 Auditory Brainstem Response (ABR) and Electrically-Evoked Auditory Brainstem Response (EABR) Testing

All testing was conducted using Tucker-Davis Technologies hardware and software. Prior to the testing, the guinea pigs were anesthetized with IM ketamine (30 mg/kg) and xylazine (5 mg/kg) administration and placed on the heating pad inside an acoustic booth. A rectal probe was inserted to monitor body temperature and maintain it around 37 °C. Otoscopic examination was performed to check the status of the outer and middle ear. Subcutaneous needle electrodes were placed between the eyes (non-inverting), below the ipsilateral pinna near the cheek (inverting), and below the contralateral pinna near the cheek (ground). Test stimuli consisted of tone bursts at 1, 2, 6, and 16 kHz (5 ms duration, 1 ms rise/fall time with Cos2 gating, 21 stimulus/sec, alternating). The speaker was placed 10 cm from the ipsilateral auditory meatus and contralateral ear was plugged with a silicon earplug. The animals' evoked responses were amplified with a gain of 5,000 and band-pass filtered from 100 Hz – 3 kHz using a Signal Recovery Model 5113 preamplifier. Responses to 300 sweeps were averaged at each stimulus level. The level of the testing signal was initially decreased in 10-dB steps from 90 dB SPL, and then in 5-dB steps to search for the threshold, defined as the lowest level at which a detectable Wave III response was elicited and repeated.

EABRs were recorded in implanted animals immediately following ABRs starting from 2 weeks after implantation. Impedance testing was performed before each session to ensure that electrodes were not open or shorted. Custom Sound EP software and external CI components (programming pod, refurbished Freedom speech processor, and implant emulator, and custom-made CI cable) were used to measure impedances and deliver electrical stimulation to the CI.

The same electrode montage and recording parameters were used as for ABR. Using the ball electrode as a ground (Monopolar 1), 300 responses to testing electrical signals (49 pulse per sec, 25 μs pulse width, 8 μs inter pulse gap, alternating current, -200 μs delay) were averaged. The electric current level was either increased or decreased in 10-CL steps (current level in microamperes (μA) on a log scale similar to dB (5.7 CL = 1 dB)) from 100 CL initially, and then 5-CL steps to search for the EABR threshold, defined as the lowest current level at which a detectable Wave II or III response was elicited and repeated.

Threshold shifts for each frequency were calculated as follows. Threshold shifts after implantation were calculated as the average ABR threshold at 2 and 4 weeks after implantation minus the average ABR threshold at baseline. Threshold shifts after chronic stimulation were calculated as the average ABR threshold after 8 and 10 weeks of stimulation (14 and 16 weeks after implantation) minus the average ABR threshold at 2 and 4 weeks after implantation.

2.6 CI Programming

The CIs in the CAES group were programmed at 5 weeks after implantation using the same external components as for EABR and clinical Custom Sound. The animals were placed inside a custom-made restraint tube (Snyder and Salvi, 1994) during programming. The Freedom speech processor was set to use monopolar stimulation (ball electrode as a ground), the Advanced Combination Encoder (ACE) processing strategy with 6 maxima (essentially chronic interleaved sampling (CIS)), 1200 pulses per second, and a 25 μs pulse width. Frequency table 6 was used to allocate the frequency range of 188 – 7938 Hz to each electrode. Impedance testing was performed before setting T- and C- levels, and only functioning electrodes were turned on. EABR thresholds were used to set T-levels, and C-levels were determined based on behavioral responses such as pinna twitching, vocalization, agitation, and teeth chattering. These behaviors were observed to make sure that the C-levels did not cause discomfort to the animals. The CI map was created by Custom Sound software and written to the speech processor. C-levels were measured and adjusted weekly to maximize the dynamic range, as is done in the clinic, and T-levels were set according to biweekly EABR measures.

2.7 Chronic Stimulation

Chronic stimulation for the CAES and CAS groups was conducted in a double-walled sound-treated booth. All animals were placed inside a custom-made restraint tube that was modified for guinea pigs (Snyder and Salvi, 1994). Up to 6 animals with restraint tubes were placed on the table in a circle. The loudspeaker was placed 37 cm above the surface of the table in the center of the circle. Amplitude modulated white noise (50% amplitude modulation, 60 dBA) was generated using MATLAB, and was used as a stimulus since it can stimulate a broad frequency range and because modulated noise is dynamic, like speech. The stimulus was presented through Microsoft Windows Player using a desktop computer and delivered simultaneously through the loudspeaker for the acoustic stimulation for both CAS and CAES animals, and an amplifier with direct audio input (DAI) connection to a Freedom speech processor for the electrical stimulation for the CAES animals only. For CAES animals, the Freedom speech processor was connected to the animal via an implant emulator and custom cable connection to the CI receptacle on the animal's head.

The level of the amplitude modulated white noise was set at 60 dBA ± 1 dB at the animal's ear level using a Brüel & Kjær sound level meter with a 1 inch microphone. This presentation level was used since it did not cause temporary or permanent threshold shift in normal-hearing guinea pigs in a pilot study.

CAES was initiated in the CAES group at 6 weeks after implantation (3 hours/day, 5 days/week) and continued for 10 weeks. For the non-implanted CAS group, only acoustic stimulation was provided for the same period of time as the CAES group. The NS guinea pigs did not receive CAES, but were placed inside the restraint tube outside of the booth (average 45.5 dBA) for the same period of time (3 hours/day, 5 days/week for 10 weeks). All animals were kept in the animal care room (average 51.5 dBA) during non-stimulation period.

2.8 Histology

After 10 weeks and final ABR/EABR measurements, all animals were euthanized with an intraperitoneal injection of sodium pentobarbital (Nembutal, 100 mg/kg) or overdosed with a ketamine-xylazine combination, and perfused intracardially with saline followed by fixative (2% glutaraldehyde in 0.15M sodium cacodylate buffer). The CI receptacle was removed from the skull of implanted animals, but the electrode array was left undisturbed in the cochlea. The location of the ball electrode was photographed and recorded. The cochlea was harvested and fixed with the same fixative overnight on a rotator.

Each cochlea was decalcified in DECAL (Decal Chemical Corp, Tallman, NY) for a week and excess bone was trimmed by micro dissection during the decalcification process. Once the decalcification was complete, images of the cochlea were taken using a Leica microscope and QCapturePro software to document ossification at the cochleostomy site. Afterward, the electrode array was removed from the cochlea. The decalcified cochlea was dehydrated in ascending concentrations of ethanol. The cochlea was infiltrated with JB-4 solution and embedded in JB-4 resin (Electron Microscopy Sciences, Washington, PA). The cochlear embeds were trimmed under a microscope to cut out excess JB-4 to the size that fits a 7-mm diameter of a beam. The trimmed embed was cemented on the beam using Quick Bond so that orientation of all cochleae would be approximately the same using the apex and round window niche as a guide.

The cochlea was serially sectioned through the mid-modiolar area at a thickness of 3 μm and a series of 40 mid-modiolar sections (3 μm/section) were collected. All mid-modiolar sections were mounted on glass slides and stained with methylene blue and basic fuchsin.

2.9 Histological analysis

The same procedures used in Kang et al. (2010) were adapted for histological analysis. Briefly, 5 sections were selected from the series of 40 mid-modiolar sections and used for histological analysis. A mid-modiolar section was defined as containing 8 profiles of the organ of Corti and at least 6 profiles of Rosenthal's Canal. Among the 40 mid-modiolar sections, five were selected for analysis in the following order: x, x+8, x+16, x+24, and x +32, where x is a random number from 1 to 8. Images of each of the 5 sections were captured using a Leica microscope and Leica Application Suite software. Figure 2 shows a light microscopic image of a mid-modiolar section of a cochlea showing different profiles (A-E) for histological analysis. Profile A is in the electrode region, profile D is about 2 kHz, and profile E corresponds to approximately 1 kHz. The quantitative data from the five sections were averaged to better estimate cochlear histology.

Following the Kang et al. (2010) definitions, cell bodies of inner and outer hair cells (IHC and OHC respectively) and spiral ganglion neurons (SGN) were counted in profiles A to E. The IHCs were counted as present if a nucleus was present, and the OHCs were counted as present if any portion of a cell body, nucleus, or stereocilia was observed. The SGN cell bodies were counted as present if the cell diameter was 12-25 μm with a nucleus between 5 and 9 μm in diameter. The Rosenthal's canal cross-sectional area was measured and SGN density was calculated as the number of SGN/Rosenthal's canal cross-sectional area (cells/mm^2). The cross-sectional area of the SV and vessel were measured to calculate vascular density (the proportion of a cross-section of SV occupied by vessels). All measures were conducted using ImageJ software. Because the cross-sectional areas of vessels are influenced by the angle of sectioning, which is very difficult to control, average values from five cochlear sections selected based on the above mentioned procedure were used to reduce potential variability introduced by angle variations. The area of fibrous tissue and dense mineralized tissue within the scala tympani in Profile A was measured using ImageJ and expressed as percent of the cross sectional area of the fibrous tissue and dense mineralized tissue relative to the scala tympani area.

2.10 Statistical Analysis

Due to the non-normal distribution of hair cell counts, a Kruskal-Wallis test followed by Dunn's test was performed to examine differences in number of hair cells (experimental group × profile). In order to examine the surgical effects on ABR thresholds, the likelihood-based mixed effects model repeated measures (MMRM) analysis was employed on the ABR threshold shits at 2 and 4 weeks after implantation relative to the baseline (pre-implantation) using group and time point as fixed (categorical) factors and baseline as a covariate. Similar analysis was performed for sound stimulation effects to examine the group difference in ABR threshold shifts at 14 and 16 weeks relative to post-implantation ABR thresholds (4 weeks after implantation).

A two-way ANOVA was used to assess group differences in pre-implantation (baseline) ABR thresholds and histological measures (experimental group × profile) for cross-sectional area of SV, SV vessels, SV density, cross-sectional area of Rosenthal's canal, number of SGNs, SGN packing density, cross-sectional area of scala tympani, and fibrous tissue. Frequency for the ABR measures and profile for the histologic measures were treated as repeated measures. Bonferroni post-hoc analyses were performed to detect which frequency or profile showed significant differences.

Linear regression analyses were performed to investigate the relationship between: 1) ABR threshold shift after implantation at 16 kHz and threshold shift after chronic stimulation at 1 kHz; 2) individual ABR threshold shifts and histological measures; 3) post-stimulation ABR threshold shift at 1 kHz and post-implantation ABR threshold shift in high frequencies. R and *p*-values from the Pearson two-tailed correlation test were calculated to evaluate a goodness of fit and slope. Due to the small sample size, Fisher's exact one-tailed test was used to investigate an association between ossification and ABR threshold shifts after implantation at 6 and 16 kHz.

3. Results

3.1 ABR Threshold Shifts after Implantation and Stimulation

Preoperative baseline ABR thresholds for all groups indicated no statistically significant differences among groups before implantation (two-way ANOVA; F=0.8273, p=0.4562; data not shown). After implantation, animals in the CAES and NS groups showed a range of threshold shifts from 0-45 dB at 6 kHz and 0-55 dB at 16 kHz, as shown in Figure 3a (CAES) and 3b (NS). The MMRM revealed a significant group effects on ABR threshold shifts at 6 kHz (F=8.52, p=0.0038) and 16 kHz (F=7.97, p=0.0049) after implantation, not at 1 kHz or 2 kHz. The post-hoc analysis revealed significant ABR threshold shifts at 6 kHz between CAES and CAS (F=14.72, p=0.0018) and NS and CAS (F=11.21, p=0.0048); at 16 kHz, CAES vs. CAS (F=15.10, p=0.0016), CAES vs. NS (F=7.21, p=0.0178). The difference in ABR thresholds after surgery between the NS and CAES is likely due to random variability in surgical outcomes across animals.

Figure 4 shows representative data from one CAES animal (n5) showing all the ABR thresholds over the experimental period. After 10 weeks (of chronic sound stimulation for the CAES or CAS groups, or restraint only for the NS group), additional threshold shifts larger than 10 dB relative to ABR thresholds after implantation were seen at 1, 2, and/or 16 kHz in some CAES animals. Thresholds shifts (difference between ABR threshold at 4 and 16 weeks after implantation) for CAS, CAES, and NS animals are shown as green, red, and blue bars in Figure 5: (a) 1 kHz; (b) 2 kHz; (c) 6 kHz; (d) 16 kHz). Of the CAES group, 4 of 6 animals showed threshold shifts of greater than 10 dB at 1 kHz and 1 animal at 2 kHz (red arrows, Figure 5a and b). The majority of CAS and NS animals did not show threshold shifts at 1 kHz; only one NS animal showed a threshold shift at 1 kHz (n26, blue arrow in Figure 5a), and this animal also happened to be the only animal with additional threshold shift at 16 kHz (Figure 5d); another NS animal showed a greater than 10 dB shift at 6 kHz (n4, blue arrow in Figure 5c). However, MMRM analysis revealed no statistically significant group effects on ABR threshold shifts after chronic sound stimulation relative to post-implantation ABR thresholds at any frequencies (data not shown). It should be noted that the one animal that showed additional HL after 10 weeks in the NS group at 1 and 16 kHz (n26) also differed from the others due to the presence of blood in the apical part of the cochlea observed at the time of cochlear collection, which might have caused changes in ABR thresholds at both 1 kHz and 16 kHz (Radeloff et al., 2007). If this animal is excluded from the analysis, then the CAES group had a significantly higher proportion of animals with more than 10 dB of HL at 1 kHz (Fisher's exact one-tailed test, p<0.05).

Because animals in the CAES group had significantly larger threshold shifts at 16 kHz after implantation than animals in the NS group, a regression analysis was performed to rule out the possibility that greater threshold shifts after surgery at 16 kHz could eventually lead to greater threshold shifts at 1 kHz after 10 weeks. Regression analysis between threshold shift after implantation at 16 kHz (difference between baseline and 4 weeks after implantation) and threshold shift after chronic stimulation at 1 kHz (difference between 4 and 16 weeks after implantation) revealed no statistically significant correlation (R=0.4378, p=0.1546,

two-tailed linear regression), which indicates that the threshold shift at 1 kHz in the CAES group is not related to the amount of hearing loss at 16 kHz developed after surgery.

3.2 Histology

3.2.1 Hair cell (HC) counts and spiral ganglion neuron (SGN) packing density

—The number of OHCs was counted in each profile in all animals, and a Kruskal-Wallis test followed by the Dunn's test revealed no significant group differences in the number of OHCs in all profiles in any group comparison. IHCs were present in all profiles in all animals. Two-way ANOVAs revealed no significant group differences in SGN packing density in any profiles in any group comparison. IHC counts, OHC counts, and SGN packing density in Profile A, which corresponds to the electrode insertion region, were not correlated with the threshold shifts after surgery in CAES and NS animals at 6 and 16 kHz (Pearson two-tailed correlation test; Figure 6a-c). Similarly, IHC counts, OHC counts, and SGN packing density in profile E, which corresponds approximately to the 1 kHz region, were not correlated with the threshold shifts in CAES animals at 1 kHz (Pearson two-tailed correlation test; n1, n5, n8, n25, n26; data not shown).

3.2.2 Stria vascularis (SV) area, blood vessel area, and blood vessel density—

Two-way ANOVAs revealed no significant group differences in SV density in any profiles in any group comparison (see example data for Profile A in Figure 6d). However, a correlation analysis of individual data from all animals plotted versus thresholds revealed a significant negative correlation between SV density in profile A (electrode region) and thresholds at 6 kHz Figure 7c, R= -0.598, p=0.009, two-tailed linear regression) and 16 kHz (Figure 7d, R= -0.511, p=0.030, two-tailed linear regression) at 16 weeks after implantation. The results indicate that higher thresholds at 6 and 16 kHz at 16 weeks after implantation are associated with lower SV densities. The majority of the CAES and NS animals had high ABR thresholds at 6 and 16 kHz and low SV densities in profile A, which corresponds to the electrode region. The overall difference in SV structure can be seen in example images for an animal with good hearing preservation and significant high-frequency hearing loss in Figures 7a and b, respectively. When the overall SV area and SV vessel areas were examined, significant correlations were also observed, suggesting that the significant effect seen for SV density is due to both increases in SV area and decreases in SV vessel area. A significant positive correlation was seen for SV area versus thresholds at 6 kHz (Figure 7e; R=0.534, p=0.029) and a significant negative correlation was seen for SV vessel area versus thresholds at 6 kHz (Figure 7f; R= -0.526, p=0.025). A significant correlation was also seen for SV vessel area versus thresholds at 16 kHz (R= -0.474, p=0.0471; not shown), but not for total SV area versus thresholds at 16 kHz (R=0.258, p=0.3; not shown).

3.2.3 Ossification at cochleostomy site—

Ossification at the electrode insertion site was observed in three CAES animals (n1, n5, and n25) and three NS animals (n9, n15, and n26). Figure 8 shows examples of ossification observed in n5 (CAES, a) and lack of ossification observed in n8 (CAES, b). In n5, the electrode array was covered by bone (black arrow) while the electrode array in n8 is clearly seen without bony coverage. No association was seen between ossification and low-frequency threshold changes at 1 kHz in n1, n5, n8, n25 due to chronic stimulation (Fisher's exact one-tailed test, p= 0.2835). However, a

significant association between ossification and high-frequency HL was observed (Fisher's exact one-tailed test, p=0.0303). Table 1 shows the classification of implanted animals based on presence of ossification and/or high-frequency HL at 6 and/or 16 kHz after implantation.

3.2.4 Fibrous and dense mineralized tissue growth—Figure 9a shows an example of fibrous tissue growth in a midmodilar section in Profile A in n9. After percent fibrous tissue area (re: scala tympani area) in Profile A was calculated, threshold shifts at 6 and 16 kHz were plotted against percent fibrous tissue area for implanted animals. Figure 9b shows a scatter plot of threshold shift after implantation at 6 and 16 kHz and fibrous tissue area (6 kHz: p = 0.327, R=0.310, 16 kHz: p = 0.536, R=0.197, two-tailed linear regression), suggesting a weak positive relationship but no statistically significant correlations between threshold shifts after surgery and fibrous tissue growth in the electrode region.

The same Profile A slides that were used in fibrous tissue analysis were used to measure blue-purple dense areas (indicative of “dense mineralized tissue”, i.e. bone or tissue in the process of transitioning to bone; MacArthur et al., 2006; Khan et al., 2000) in the scala tympani. The percentage of dense mineralized tissue area (re: scala tympani area) was very low in Profile A for most animals (less than 5% for all animals except n5), and showed no correlation with high frequency threshold shifts (R=39, p=0.21; not shown).

4. Discussion

4.1 Normal-Hearing Guinea Pig Model of Hybrid Cochlear Stimulation

All implanted animals experienced a range of 0-55 dB of threshold shifts in the vicinity of the electrode at 6 and 16 kHz after surgery. After 10 weeks of stimulation, more implanted, stimulated animals (CAES) had an additional 10 dB of threshold shift at 1 kHz, compared to implanted, non-stimulated animals (NS). The variation in degree of hearing loss after implantation surgery in this animal model is consistent with the variation in human Hybrid CI patients. This contrasts with other animal CI studies in which near-total rather than partial hearing loss was observed after surgery alone. Further, we were able to replicate the delayed hearing loss seen in some human patients in the electrically stimulated animals. These two factors indicate the suitability of this animal model and stimulation paradigm as a model for human Hybrid CIs.

These findings also illustrate an advantage of a normal-hearing animal model over a hearing-impaired model generated via chemical deafening or noise exposure. In the absence of pre-existing hearing loss, the damage induced by implantation can be directly measured as changes in hearing thresholds as well as through histology without questions of whether the damage arose due to the pre-existing hearing loss.

Previous studies (Coco et al., 2007; Ni et al., 1992; Shepherd et al., 1983; Xu et al., 1997) used normal-hearing animals and reported that electrical stimulation had no effect on residual low-frequency hearing, which is inconsistent with the current study. The low-frequency hearing loss observed after 10 weeks of acoustic and electric stimulation in the current study may be due to differences in current densities from customized CI mapping, or the use of combined acoustic and electrical stimulation.

While the use of normal-hearing animals gives useful information due to lack of the confound effects of an existing hearing loss, use of animals with hearing impairment is equally important since it simulates human CI users. The majority of studies that studied hearing impaired animals with CIs used chemical deafening to induce hearing loss because of its relatively quick effects. However, etiology of hearing loss in human CI users is not limited to ototoxic-drug exposure. Future study may need to explore other partial deafening procedures such as noise-induced hearing loss or usage of animals with generic disorders to study the effects of hybrid CIs on residual hearing.

4.2 Histological Correlates of Post-Surgical High-Frequency Hearing Loss

Five CAES and three NS animals showed high-frequency threshold shifts immediately after surgery. Thus, these animals provided an opportunity to correlate histological measures with HL due to surgery itself. Surprisingly, no significant effect of implantation was observed on IHC, OHC, or SGN counts or densities. The lack of hair cell loss in this study is consistent with Kang et al. (2010) who reported postoperative hearing loss at 8 and 24 kHz an implanted normal-hearing guinea pig, but no corresponding HC or SGN pathology. They proposed that this may be due to HC or SGN pathology not revealed in a light microscope examination or to mechanical disruption of basilar membrane motion due to the presence of the electrode array. Other studies, however, have reported progressive hearing loss and hair cell loss due to insertion trauma during cochlear implantation surgery (Eshraghi et al., 2005; Vivero et al., 2008). However, these studies differed from the current study in that they induced more severe hearing loss after insertion trauma, unlike the moderate degree of hearing loss observed in this study. Thus, one reason for the inconsistency may be that hair cell loss only occurs with more severe insertion trauma. In addition, one limitation of the cochlear mid-modiolar section approach used in the current study is the limited number of sections that can be analyzed. Future studies will warrant the use of a cochlear whole mount for more in depth analysis of hair cell loss in relation to residual hearing loss.

The lack of effects of electrical stimulation on SGC survival are consistent with studies showing no effect of electrical stimulation (Li et al., 1999; Shepherd et al., 2005; Agterberg et al., 2010), but differ from other studies which reported protective effects on SGN packing density (Lousteau, 1987; Hartshorn et al., 1991; Miller and Altschuler, 1995; Mitchell et al., 1997; Kanzaki et al., 2002; Miller et al., 2003; Scheper et al., 2009).

Although our study did not find loss of IHC, OHC, or decreased SGN counts or densities, we did find statistically significant correlations between SV vascular density in profile A and post-surgical threshold shifts at 6 and 16 kHz in all implanted animals. These findings suggest that changes in blood circulation in the basal turn of the cochlea and a resulting reduction of endocochlear potential may be more important contributors to post-surgical HL than HC or SGN survival. This is the first study to look at the effects of implantation on SV in an animal model, and the data obtained indicate that further study of these effects are warranted, as damage to the SV may be an under-investigated mechanism for surgical-trauma-induced implantation HL. Certainly the involvement of the SV in damage mechanisms is not surprising given its vulnerable position along the lateral wall (Wright and

Roland, 2013) and the electrode insertion trajectory, especially for a straight electrode design.

On the other hand, a significant association between ossification at the cochleostomy site and post-surgical high-frequency HL was also observed in our study. A study by Richard et al. (2012) in human temporal bones found more new bone formation and cochlear hydrops in the scala tympani of the basal turn with an enlarged round window or cochleostomy approach, compared to a round window insertion. If new bone formation contributes to HL, insertion through the RW may be a better approach for minimizing post-surgical HL.

Unlike our study which found no significant correlation between fibrosis area and post-surgical hearing loss, the recent study by O'Leary's et al. (2013) reported a significant correlation between fibrosis and the recovery of ABR thresholds in 73 implanted guinea pigs. Similarly, in our study, no correlation was seen between mineralized tissue (bone or tissue in the process of transitioning to bone) within the scala tympani and post-surgical hearing loss. The discrepancy between two studies could be largely due to differences in the number of subjects, or due to the fibrosis and mineralized tissue measurements being conducted at the electrode region rather than the cochleostomy region.

While both SV vessel density and ossification were found to be associated with high-frequency post-implantation HL, this does not necessarily imply a causal relationship of both to the HL. It may be that the HL, SV vessel density, and ossification are all associated because of a causal relationship to another as-yet uncovered histological variable. Alternatively, it may be that either SV changes or ossification alone are responsible for HL. For example, surgical trauma to the SV may directly reduce the endocochlear potential, but also have the side effect of inducing tissue repair pathways including osteogenesis and fibrogenesis. Alternatively, ossification may affect the traveling wave, and also impact the health of the SV. Further studies are needed to separate these effects and clarify why these variables are associated with post-surgical HL.

4.2 Residual Hearing Loss at 1 kHz

The current study also investigated whether chronic electric and acoustic stimulation could cause the delayed low-frequency residual hearing loss previously reported in Hybrid or EAS cochlear implant recipients (Gantz et al., 2009; Gstoettner et al., 2009; Santa Maria et al., 2013). Due to the limited number of animals with large variability in residual hearing loss, we did not observe statistically significant group differences in threshold shifts at 1 kHz after chronic stimulation between the CAES and NS groups. However, a higher proportion of 4 of 6 of the CAES animals (n1, n5, n8, and n25) showed greater than 10 dB threshold shift at 1 kHz due to chronic stimulation while only 1 of 6 the NS animals (n26, which differs from the other NS animals because of the presence of blood in the cochlea and additional high-frequency HL) showed greater than 10 dB threshold shift at 1 kHz in the absence of chronic stimulation during the same period of time. The results imply that chronic stimulation may be, in part, contributing to development of residual HL in some animals. The variability in the HL across animals is also consistent with the variability of HL seen in human patients, of which approximately 30% exhibited delayed post-activation HL.

We did not find an association of post-stimulation threshold shifts at 1 kHz with the amount of high-frequency threshold shift that occurred right after implantation. However, the lack of a significant effect does not rule out a possibility that effects from both surgery and electrical stimulation could contribute to delayed development of residual HL at 1 kHz. For future studies, it would be ideal to have two groups of CAES animals with and without high-frequency HL after surgery to isolate the effects of electrical stimulation on residual HL from surgical effects.

Surprisingly, no correlation was found between residual HL at 1 kHz and any of our histological analyses. No IHC loss was observed in any animals. Some OHC loss was observed in profile E in limited numbers of the animals (CAES: n24; NS: n9 and n15), but these animals were not the ones that showed residual hearing changes at 1 kHz after chronic stimulation. The lack of hair cell loss observed in our study is consistent with Coco et al. (2007), which showed no significant changes in hair cell survival after chronic electrical stimulation. Neither SGN packing density nor SV density was associated with residual hearing loss at 1 kHz.

It is possible that the etiology of the residual HL in the Hybrid CI recipients may not be something that could be detected under a light microscope. For instance, one likely etiology would be over-excitation from the electrical stimulation. While the acoustic stimulation was conducted at a known safe level for acoustic-only stimulation at 60 dB SPL, little is known about safe levels for combined electric and acoustic stimulation. Certainly, noise-induced HL is known to be caused by glutamate excitotoxicity in IHCs (Puel et al, 1998; Kujawa and Liberman, 2009; Wang and Green, 2011). Lin et al. (2011) reported that IHC synapses and cochlear nerve terminals are degenerated after traumatic noise exposure. A potential future study would be to use immunolabeling techniques to assess synaptic damage at IHCs in implanted guinea pigs after electro-acoustic stimulation.

5. Conclusions

The replication of the range of hearing loss both after surgery and after electrical stimulation in normal-hearing guinea pigs demonstrates its suitability as a model for investigation of the mechanisms of hearing loss in human Hybrid CI patients. This study is also the first study to support a role of the stria vascularis and/or formation of new bone around the electrode, in implantation-induced hearing loss, and indicates the need for more detailed investigation in these directions. Further investigation is necessary, however, to conclude a strong association between low frequency residual hearing loss and electrical stimulation, and to find physiological correlates for the electrical-stimulation induced hearing loss. Clearly, in order to eventually develop treatments or strategies to prevent hearing loss after implantation, further study of mechanisms of both low-frequency hearing loss from chronic stimulation and high-frequency hearing loss from surgical trauma is needed.

Acknowledgments

This study was funded by a NIH-NIDCD grant P30DC010755, a NCRR grant KL2RR024141, and a NIH-NIDCD grant P30DC005983 to the Oregon Hearing Research Center (OHRC). The authors thank Yehoash Raphael and his lab members at Kresge Hearing Research Institute for cochlear histology training; Dennis Trune for cochlear histology consultation and for helpful comments on the manuscript, Xiao-Rui Shi and their lab members at OHRC

and Dalian Ding at State University of New York at Buffalo for cochlear histology consultation; Paul Abbas and Carolyn Brown at the University of Iowa, and Manuel Don and Mickey Waring for electrophysiology consultation; and John Brigande and his lab members at the OHRC in assistance in cochlear imaging. The authors also thank Michael Reiss for help with custom cochlear implant assembly design; Richard Salvi at State University of New York at Buffalo for providing information for the custom-made animal restraint; David Wozny for building the restraint; Frank Risi at Cochlear for assistance with obtaining external cochlear implant components; Guang-Di Chen at State University of New York at Buffalo for providing ABR loudspeakers; Edward Porsov and Fangyi Chen at OHRC for troubleshooting equipment problems; Judy Jin for assistance in statistical analysis.

References

Agterberg MJ, Versnel H, de Groot JC, van den Broek M, Klis SF. Chronic electrical stimulation does not prevent spiral ganglion cell degeneration in deafened guinea pigs. Hear Res. 2010; 269:169–79. [PubMed: 20600740]

Briggs RJ, Tykocinski M, Stidham K, Roberson JB. Cochleostomy site: implications for electrode placement and hearing preservation. Acta Otolaryngol. 2005; 125:870–6. [PubMed: 16158535]

Ching TY, Dillon H, Byrne D. Speech recognition of hearing-impaired listeners: predictions from audibility and the limited role of high-frequency amplification. J Acoust Soc Am. 1998; 103:1128–40. [PubMed: 9479766]

Choi CH, Oghalai JS. Predicting the effect of post-implant cochlear fibrosis on residual hearing. Hear Res. 2005; 205:193–200. [PubMed: 15953528]

Coco A, Epp SB, Fallon JB, Xu J, Millard RE, Shepherd RK. Does cochlear implantation and electrical stimulation affect residual hair cells and spiral ganglion neurons? Hear Res. 2007; 225:60–70. [PubMed: 17258411]

Eshraghi AA, Polak M, He J, Telischi FF, Balkany TJ, Van De Water TR. Pattern of hearing loss in a rat model of cochlear implantation trauma. Otol Neurotol. 2005; 26:442–7. discussion 447. [PubMed: 15891647]

Eshraghi AA, Gupta C, Van De Water TR, Bohorquez JE, Garnham C, Bas E, Talamo VM. Molecular mechanisms involved in cochlear implantation trauma and the protection of hearing and auditory sensory cells by inhibition of c-Jun-N-terminal kinase signaling. Laryngoscope. 2013; 123(Suppl 1):S1–14. [PubMed: 23382052]

Gantz BJ, Turner CW. Combining acoustic and electrical hearing. Laryngoscope. 2003; 113:1726–30. [PubMed: 14520097]

Gantz BJ, Hansen MR, Turner CW, Oleson JJ, Reiss LA, Parkinson AJ. Hybrid 10 clinical trial: preliminary results. Audiol Neurootol. 2009; 14(Suppl 1):32–8. [PubMed: 19390173]

Gfeller KE, Olszewski C, Turner C, Gantz B, Oleson J. Music perception with cochlear implants and residual hearing. Audiol Neurootol. 2006; 11(Suppl 1):12–5. [PubMed: 17063005]

Greenwood DD. A cochlear frequency-position function for several species--29 years later. J Acoust Soc Am. 1990; 87:2592–605. [PubMed: 2373794]

Gstoettner W, Helbig S, Settevendemie C, Baumann U, Wagenblast J, Arnoldner C. A new electrode for residual hearing preservation in cochlear implantation: first clinical results. Acta Otolaryngol. 2009; 129:372–9. [PubMed: 19140036]

Hartshorn DO, Miller JM, Altschuler RA. Protective effect of electrical stimulation in the deafened guinea pig cochlea. Otolaryngol Head Neck Surg. 1991; 104:311–9. [PubMed: 1902931]

Hogan CA, Turner CW. High-frequency audibility: benefits for hearing-impaired listeners. J Acoust Soc Am. 1998; 104:432–41. [PubMed: 9670535]

Kamm CA, Dirks DD, Bell TS. Speech recognition and the Articulation Index for normal and hearing-impaired listeners. J Acoust Soc Am. 1985; 77:281–8. [PubMed: 3973220]

Kang SY, Colesa DJ, Swiderski DL, Su GL, Raphael Y, Pfingst BE. Effects of hearing preservation on psychophysical responses to cochlear implant stimulation. J Assoc Res Otolaryngol. 2010; 11:245–65. [PubMed: 19902297]

Kanzaki S, Stover T, Kawamoto K, Prieskorn DM, Altschuler RA, Miller JM, Raphael Y. Glial cell line-derived neurotrophic factor and chronic electrical stimulation prevent VIII cranial nerve degeneration following denervation. J Comp Neurol. 2002; 454:350–60. [PubMed: 12442325]

Khan DC, DeGagne JM, Trune DR. Abnormal cochlear connective tissue mineralization in the palmerston north autoimmune mouse. Hear Res. 2000; 142:12–22. [PubMed: 10748324]

Kiefer, J.; Tillein, J.; von Ilberg, C.; Pfennigdorff, T.; Sturzebecher, E.; Klinke, R.; Gstottner, W. Fundamental aspects and first clinical results of the clinical application of combined electric and acoustic stimulation of the auditory system. In: Kubo, T.; Takahashi, Y.; Iwaki, T., editors. Advances in Cochlear Implants - An Update. Kugler Publications; The Hague: 2002. p. 569-576.

Kujawa SG, Liberman MC. Adding insult to injury: cochlear nerve degeneration after “temporary” noise-induced hearing loss. J Neurosci. 2009; 29:14077–85. [PubMed: 19906956]

Li L, Parkins CW, Webster DB. Does electrical stimulation of deaf cochleae prevent spiral ganglion degeneration? Hear Res. 1999; 133:27–39. [PubMed: 10416862]

Lin HW, Furman AC, Kujawa SG, Liberman MC. Primary neural degeneration in the Guinea pig cochlea after reversible noise-induced threshold shift. J Assoc Res Otolaryngol. 2011; 12:605–16. [PubMed: 21688060]

Lousteau RJ. Increased spiral ganglion cell survival in electrically stimulated, deafened guinea pig cochleae. Laryngoscope. 1987; 97:836–42. [PubMed: 3600136]

MacArthur CJ, Hefeneider SH, Kempton JB, Trune DR. C3H/HeJ mouse model for spontaneous chronic otitis media. Laryngoscope. 2006; 116:1071–9. [PubMed: 16826039]

Miller JM, Altschuler RA. Effectiveness of different electrical stimulation conditions in preservation of spiral ganglion cells following deafness. Ann Otol Rhinol Laryngol Suppl. 1995; 166:57–60. [PubMed: 7668758]

Miller AL, Prieskorn DM, Altschuler RA, Miller JM. Mechanism of electrical stimulation-induced neuroprotection: effects of verapamil on protection of primary auditory afferents. Brain Res. 2003; 966:218–30. [PubMed: 12618345]

Mitchell A, Miller JM, Finger PA, Heller JW, Raphael Y, Altschuler RA. Effects of chronic high-rate electrical stimulation on the cochlea and eighth nerve in the deafened guinea pig. Hear Res. 1997; 105:30–43. [PubMed: 9083802]

Ni D, Shepherd RK, Seldon HL, Xu SA, Clark GM, Millard RE. Cochlear pathology following chronic electrical stimulation of the auditory nerve. I: Normal hearing kittens. Hear Res. 1992; 62:63–81. [PubMed: 1429252]

O'Leary MJ, Fayad J, House WF, Linthicum FH Jr. Electrode insertion trauma in cochlear implantation. Ann Otol Rhinol Laryngol. 1991; 100:695–9. [PubMed: 1952658]

O'Leary SJ, Monksfield P, Kel G, Connolly T, Souter MA, Chang A, Marovic P, O'Leary JS, Richardson R, Eastwood H. Relations between cochlear histopathology and hearing loss in experimental cochlear implantation. Hear Res. 2013; 298:27–35. [PubMed: 23396095]

Pavlovic CV. Use of the articulation index for assessing residual auditory function in listeners with sensorineural hearing impairment. J Acoust Soc Am. 1984; 75:1253–8. [PubMed: 6725776]

Puel JL, Ruel J, Gervais d'Aldin C, Pujol R. Excitotoxicity and repair of cochlear synapses after noise-trauma induced hearing loss. Neuroreport. 1998; 9:2109–14. [PubMed: 9674603]

Radeloff A, Unkelbach MH, Tillein J, Braun S, Helbig S, Gstottner W, Adunka OF. Impact of intrascalar blood on hearing. Laryngoscope. 2007; 117:58–62. [PubMed: 17202931]

Richard C, Fayad JN, Doherty J, Linthicum FH Jr. Round window versus cochleostomy technique in cochlear implantation: histologic findings. Otol Neurotol. 2012; 33:1181–7. [PubMed: 22892806]

Roland PS, Wright CG. Surgical aspects of cochlear implantation: mechanisms of insertional trauma. Adv Otorhinolaryngol. 2006; 64:11–30. [PubMed: 16891834]

Santa Maria PL, Domville-Lewis C, Sucher CM, Chester-Browne R, Atlas MD. Hearing preservation surgery for cochlear implantation--hearing and quality of life after 2 years. Otol Neurotol. 2013; 34:526–31. [PubMed: 23503094]

Scheper V, Paasche G, Miller JM, Warnecke A, Berkingali N, Lenarz T, Stover T. Effects of delayed treatment with combined GDNF and continuous electrical stimulation on spiral ganglion cell survival in deafened guinea pigs. J Neurosci Res. 2009; 87:1389–99. [PubMed: 19084902]

Shepherd RK, Clark GM, Black RC. Chronic electrical stimulation of the auditory nerve in cats. Physiological and histopathological results. Acta Otolaryngol Suppl. 1983; 399:19–31. [PubMed: 6316712]

Shepherd RK, Coco A, Epp SB, Crook JM. Chronic depolarization enhances the trophic effects of brain-derived neurotrophic factor in rescuing auditory neurons following a sensorineural hearing loss. J Comp Neurol. 2005; 486:145–58. [PubMed: 15844207]

Snyder DL, Salvi RJ. A novel chinchilla restraint device. Lab Animal. 1994; 24:42–44.

Turner C, Gantz BJ, Reiss L. Integration of acoustic and electrical hearing. J Rehabil Res Dev. 2008; 45:769–78. [PubMed: 18816425]

Turner CW, Gantz BJ, Vidal C, Behrens A, Henry BA. Speech recognition in noise for cochlear implant listeners: benefits of residual acoustic hearing. J Acoust Soc Am. 2004; 115:1729–35. [PubMed: 15101651]

Vivero RJ, Joseph DE, Angeli S, He J, Chen S, Eshraghi AA, Balkany TJ, Van de Water TR. Dexamethasone base conserves hearing from electrode trauma-induced hearing loss. Laryngoscope. 2008; 118:2028–35. [PubMed: 18818553]

Wang Q, Green SH. Functional role of neurotrophin-3 in synapse regeneration by spiral ganglion neurons on inner hair cells after excitotoxic trauma in vitro. J Neurosci. 2011; 31:7938–49. [PubMed: 21613508]

Wilson BS, Lawson DT, Muller JM, Tyler RS, Kiefer J. Cochlear implants: some likely next steps. Annu Rev Biomed Eng. 2003; 5:207–49. [PubMed: 12704085]

Wright CG, Roland PS. Vascular trauma during cochlear implantation: a contributor to residual hearing loss? Otol Neurotol. 2013; 34:402–7. [PubMed: 23222961]

Xu J, Shepherd RK, Millard RE, Clark GM. Chronic electrical stimulation of the auditory nerve at high stimulus rates: a physiological and histopathological study. Hear Res. 1997; 105:1–29. [PubMed: 9083801]

Abbreviations

ABR	Auditory brainstem response
ACE	Advanced Combination Encoder
CAES	Chronic Acoustic Electric Stimulation
CAS	Chronic Acoustic Stimulation
CI	Cochlear implant
CIS	Chronic interleaved sampling
EABR	Electrically-evoked auditory brainstem response
EAS	Electric and acoustic stimulation
HA	Hearing Aid
HC	Hair cell
HL	Hearing loss
IHC	Inner hair cell
IM	Intramuscular
NS	No stimulation
OHC	Outer hair cell
SGN	Spiral ganglion neuron
SV	Stria vascularis, stria vascular

Highlights

- Hearing loss after implantation was associated with reduced stria vascular density
- Hearing loss after implantation was also associated with ossification
- Additional hearing loss occurred in 67% of cases after electro-acoustic stimulation
- Hearing loss was not associated with hair cell or spiral ganglion measures

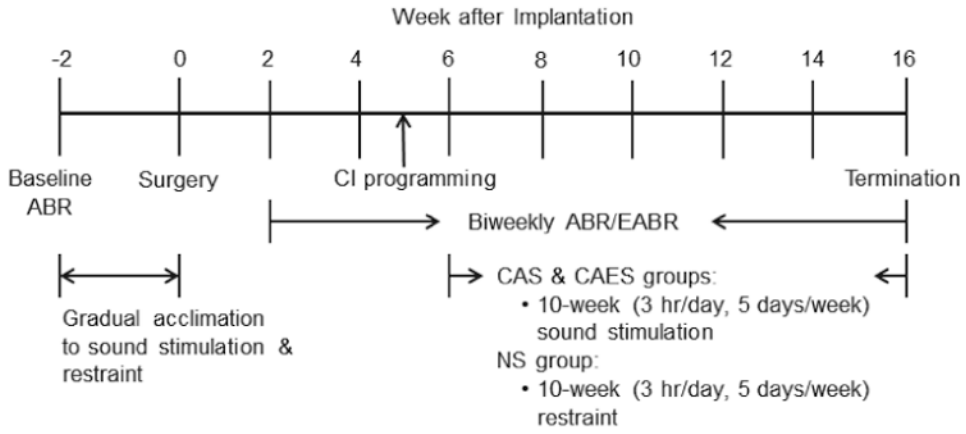

Figure 1.
Study timeline.

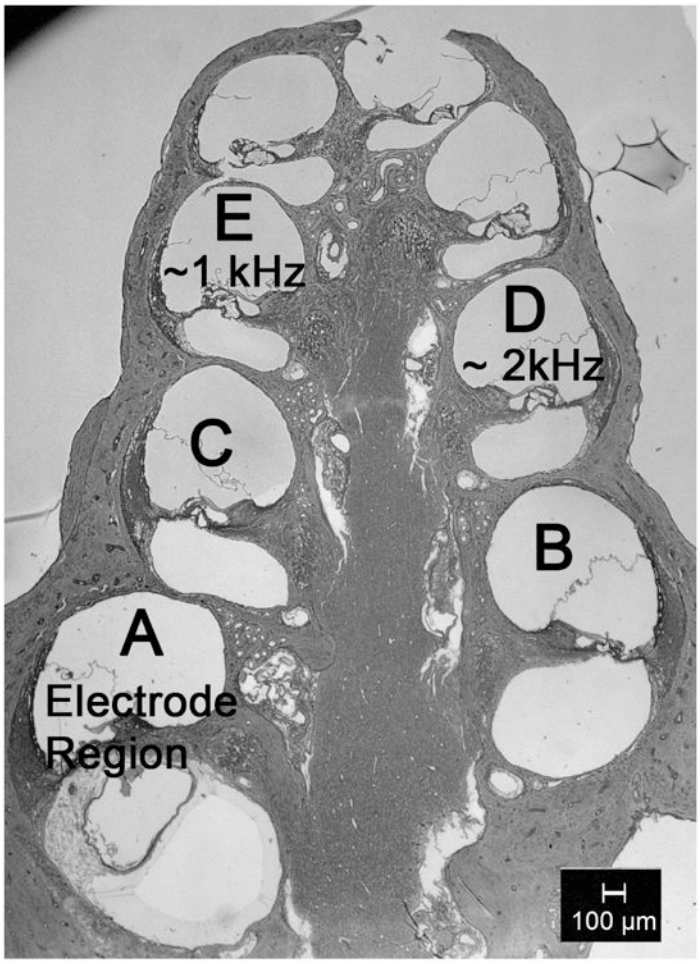

Figure 2.

A light microscopic image of a mid-modiolar section of a cochlea showing different profiles (A-E) for histological analysis.

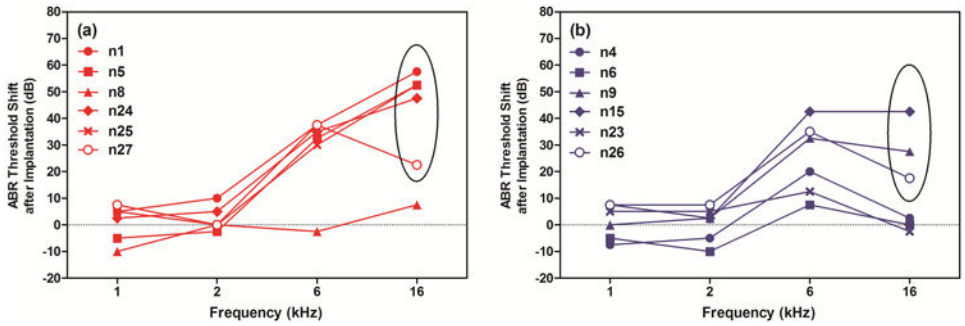

Figure 3.

ABR threshold shifts after implantation at 1, 2, 6, and 16 kHz for animals in the CAES (a) and NS (b) groups. Threshold shifts ranged from 0-45 dB at 6 kHz and 0-55 dB at 16 kHz. Five CAES animals showed greater than 10 dB ABR threshold shift at 16 kHz after surgery (n1, n5, n24, n25, and n27) and three NS animals showed greater than 10 dB of threshold shift at 16 kHz after surgery in the NS group (n9, n15, and n26).

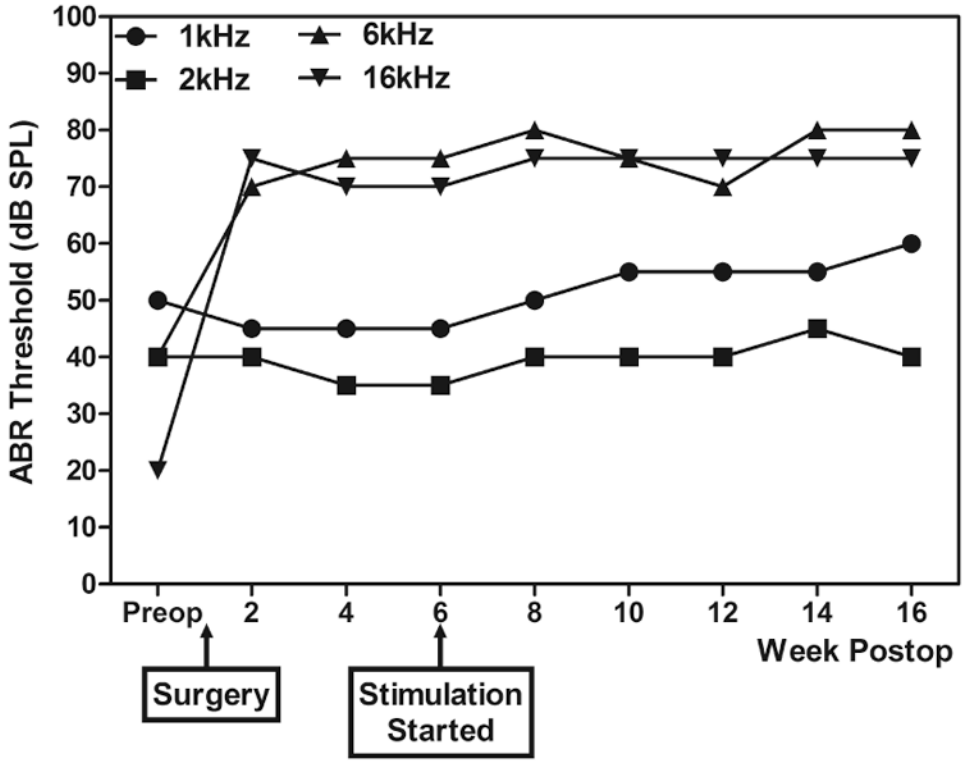

Figure 4.

Representative data from CAES animal (n5) showing all the ABR thresholds over the experimental period. This animal showed additional 15-dB threshold shifts at 1 kHz at 16 weeks after implantation (after 10 weeks of chronic sound stimulation) at 1 kHz relative to the ABR threshold at 4 weeks after implantation.

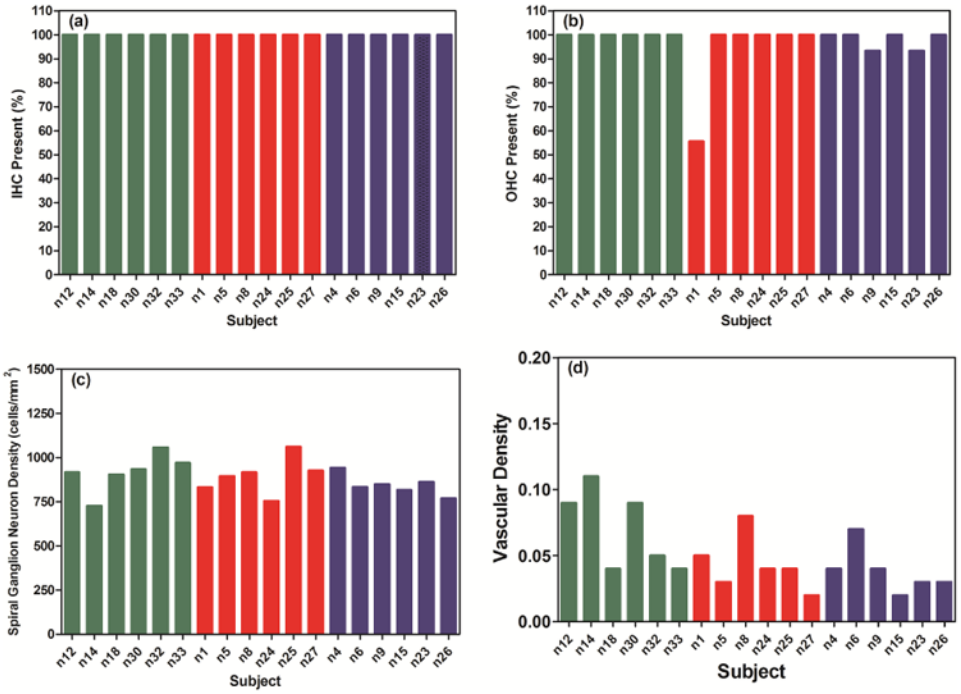

Figure 5.

Additional threshold shifts after 10 weeks of chronic stimulation at 1 kHz (a), 2 kHz (b), 6 kHz (c), and 16 kHz (d) by individual animals. Arrows indicate >10 dB ABR threshold shift. The ABR threshold shifts show ABR threshold difference between ABR threshold at 4 and 16 weeks after implantation.

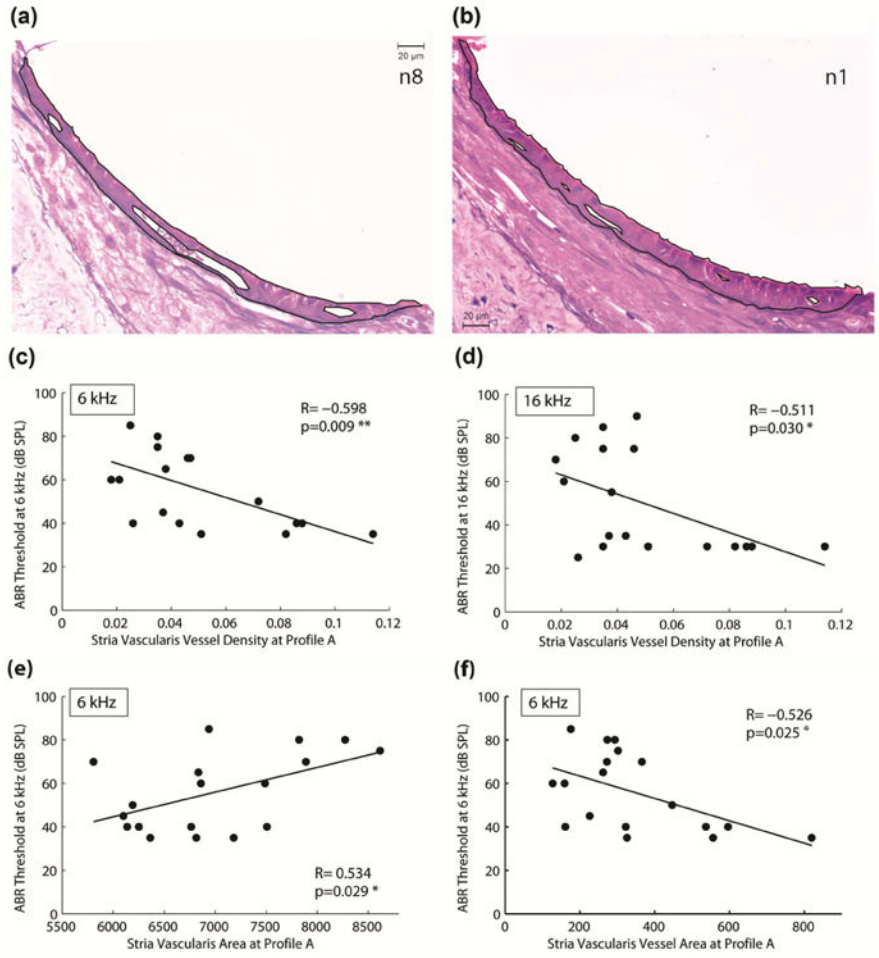

Figure 6.

Percentage of IHC (a) and OHC (b) present, spiral ganglion neuron (SGN) density (c), and stria vascular (SV) density (d) in Profile A (electrode region). Only stria vascular density was associated with the high-frequency threshold shifts as shown in Figure 7.

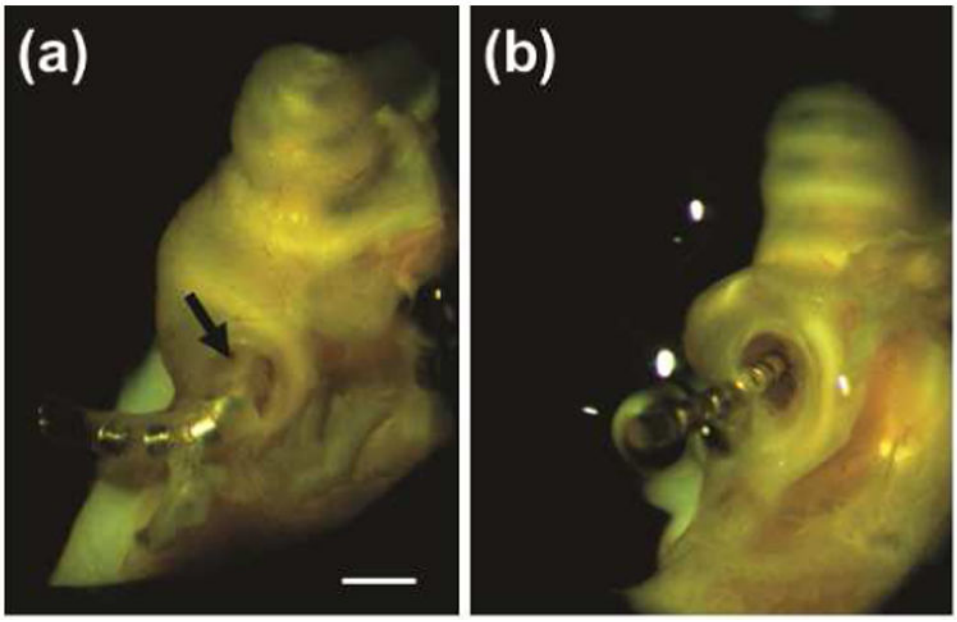

Figure 7.

Stria vascularis measures. (a) Example digitized light microscopic image of the SV for an implanted animal without hearing loss (n8). (b) Example image of the SV for an implanted animal with hearing loss (n1). Black lines indicate borders of stria vascularis and vessels used for vascular density measurements (the proportion of stria vascularis occupied by vessels). (c) Statistically significant linear correlations between ABR threshold at 6 kHz at 16 weeks after implantation and SV vascular density in profile A (R= -0.598, p=0.009). (d) Statistically significant linear correlations between ABR threshold at 16 kHz at 16 weeks after implantation and vascular density in profile A (R= -0.511, p=0.030). Significant linear correlations indicated that the lower the vascular density in the CI electrode region, the more hearing loss was detected at 6 k and 16 kHz. (e) A significant positive correlation was also seen for total SV area versus ABR threshold at 6 kHz (R=0.534, p=0.029). This indicated that the higher the SV area in the electrode region, the more hearing loss was detected at 6 kHz. (f) A significant negative correlation was also seen for total SV blood vessel area versus ABR threshold at 6 kHz (R= -0.526, p=0.025). This indicates that smaller overall blood vessel size was associated with more hearing loss at 6 kHz.

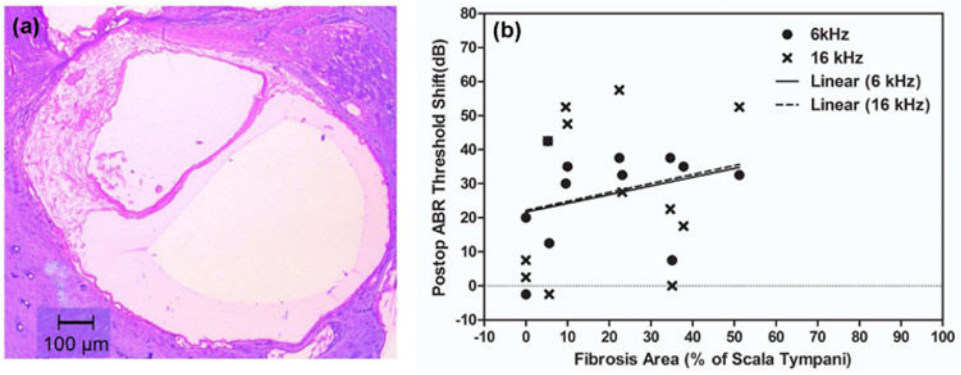

Figure 8.

Example images of cochleae with and without ossification at the cochleostomy site. (a) n5 in the CAES group, showing ossification at cochleostomy site (black arrow). (b) n8 in the NS group without ossification. Note that the electrode array can be seen clearly in this cochlea.

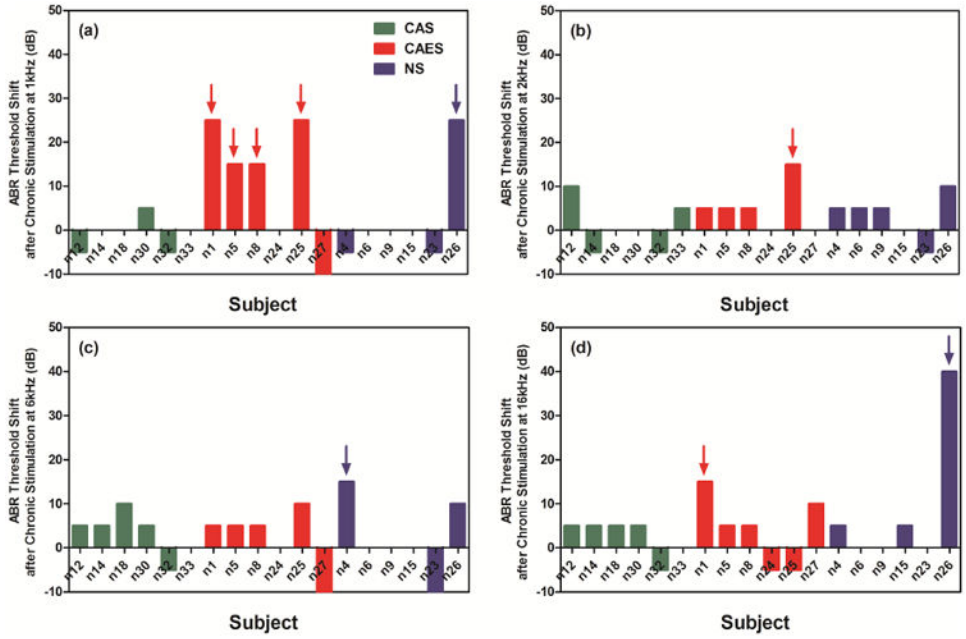

Figure 9.

Fibrosis quantification results. (a) An example of fibrous tissues in a mid-modiolar section in Profile A in n9. (b) A scatter plot of ABR threshold shifts at 6 and 16 kHz after implantation versus percent fibrous tissue area (re: scala tympani area) in profile A for all implanted animals. No significant correlation was seen between fibrosis area and high frequency HL.

Table 1

Implanted animals classified based on presence of ossification and/or high-frequency hearing loss (HFHL) at 6 and/or 16 kHz after implantation. A significant association between ossification and high-frequency HL was observed (Fisher's exact one-tailed test, p=0.0303). No association was seen between ossification and low-frequency HL.

Number of Animals	HFHL	No HFHL	Total
Ossification	6	0	6
No Ossification	2	4	6
Total	8	4	12